Analysis of the Anisotropy of Finite Difference Schemes

M.E. Young[1] **and A. Ooi**[2]

[1]Air Vehicles Division
Defence Science and Technology Organisation, Fishermans Bend, Victoria 3207, Australia

[2]Department of Mechanical Engineering
University of Melbourne, Parkville, Victoria 3052, Australia

Abstract

Numerical differencing schemes are subject to dispersive and dissipative errors, which in one dimension are functions of wavenumber. When these schemes are applied in two or three dimensions, the errors become functions of both wavenumber and the direction of wave propagation. Spectral analysis and numerical examples using the scalar advection equation are used to assess two finite difference schemes on two-dimensional grids of varying aspect ratio. It is shown that waves can not only propagate at the wrong speed—as per the dispersive errors seen in the one dimensional case—but also in the wrong direction.

Introduction

This paper outlines the calculation of group velocity using spectral analysis, then uses this analysis to predict the propagation of waves advecting over a two-dimensional grid using different finite difference schemes. The aspect ratio of the grid, $\lambda = \Delta_y/\Delta_x$, and the angle of propagation are varied. These predictions are then compared to the results of numerical experiments and the exact solution.

The use of spectral analysis (also called wavenumber or Fourier analysis) in computational numerics is well established; therefore, this paper will not discuss the underlying theory in detail, deferring to the treatments given elsewhere such as [4] and [9].

Much of the literature using spectral analysis is only applied in one dimension (e.g. [7]). However, in two dimensions the resolution of a numerical scheme is no longer only a function of wavenumber, but it is also dependent on the angle of wave propagation. Therefore, if we naively extend the one dimensional analysis to two or three dimensions, we omit important information regarding the dependence that dispersion has on wave propagation direction. Even papers that deal with anisotropy, e.g. [2, 3, 6], are of somewhat limited scope, restricting themselves to assessing phase velocity rather than group velocity and not addressing the direction issue.

It is shown herein that the polar plots of phase speed that are conventionally used to show the anisotropy in two-dimensional cases cannot explain the phenomena observed, and that the use of group velocity as determined via the spectral analysis correctly predicts the location of the wave.

Finite Difference Schemes

Finite difference schemes can be divided into three broad categories: conventional central or upwind difference schemes; compact (or Padé) schemes as introduced by Lele [2]; and the 'dispersion relation preserving' (DRP) (or similarly optimised) schemes as introduced by Tam and Webb [7]. For the purposes of exploring the anisotropy of finite difference schemes, examples from the first two categories were selected for analysis. They are the fourth order central difference scheme (CDS4):

$$\phi_i' = \frac{\phi_{i-2} - 8\phi_{i-1} + 8\phi_{i+1} - \phi_{i+2}}{12\Delta}; \qquad (1)$$

and the sixth order compact difference scheme (COM6):

$$\alpha\phi_{i-1}' + \phi_i' + \alpha\phi_{i+1}' = b\frac{\phi_{i+2} - \phi_{i-2}}{4\Delta} + a\frac{\phi_{i+1} - \phi_{i-1}}{2\Delta} \qquad (2)$$

where $\alpha = \frac{1}{3}$, $a = \frac{14}{9}$, and $b = \frac{1}{9}$. Δ is the grid spacing and ϕ is a scalar quantity.

Spectral Analysis

Spectral analysis can tell us the wavenumber range that a numerical scheme can accurately resolve. In order to illustrate this, the concept of equivalent wavenumber can be used to show the relationship between the exact wavenumber, k, and the numerical equivalent, k^*. The equivalent wavenumber for the spatial semi-discretisations using the schemes listed above, are

$$(k^*\Delta)_{\text{CDS4}} = \frac{4}{3}\sin(k\Delta) - \frac{1}{6}\sin(2k\Delta); \qquad (3)$$

$$(k^*\Delta)_{\text{COM6}} = \frac{a\sin(k\Delta) + \frac{b}{2}\sin(2k\Delta)}{1 + 2\alpha\cos(k\Delta)}; \qquad (4)$$

where the coefficients are as noted for equation (2) above.

When plotted as in figure 1, the equivalent wavenumber of all schemes approximates the exact solution at low wavenumber. As wavenumber increases, the schemes start to drop off at different points. The longer the scheme approximates the 'exact' relationship, the better its resolution properties. Whilst the effects of temporal discretisation must be taken into account as well, this relationship essentially determines the phase velocity, group velocity, amplification (or attenuation) factor, and dissipation of a numerical scheme.

Many previous analyses (e.g. [3] and [6]) either neglect or omit the effects of temporal discretisation. Whilst such effects are not necessarily negligible they will not be dealt with here. Instead, the examples that follow all have a Courant (CFL) number small enough so that they are effectively equal to the semi-discretisation case, as per [9], which showed how the dispersion relation of the full-discretisation approaches the dispersion relation of the spatial semi-discretisation as the timestep approaches zero.

A typical assessment of the anisotropy of a numerical scheme will consist of a plot such as the one shown in figure 2. This shows how, as the angle of propagation, θ, varies, the ratio of numerical to exact phase speed changes, thereby illustrating the anisotropic behaviour of the scheme. However, implicit in such a figure is the assumption that the wave is aligned with the direction of propagation, which requires that the frequency content of the wave be such that $k_y/k_x = \Delta_y/\Delta_x = \tan(\theta)$. Whilst the linearised Euler and shallow water equations, for example, have axisymmetric solutions for which the above is true; this is not necessarily the general case [1]. Consider a wave aligned with $\theta = 0$ degrees, under the advection equation, this can be propagated in any direction. Furthermore, this style of figure only
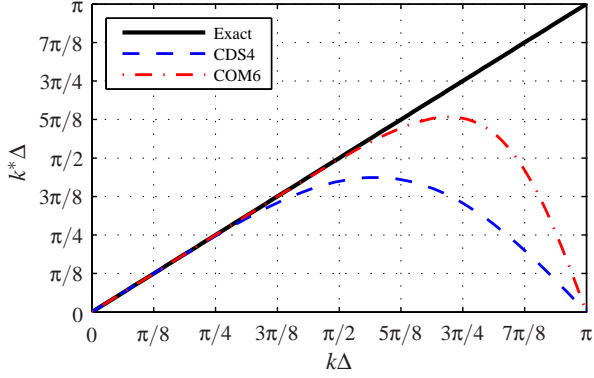
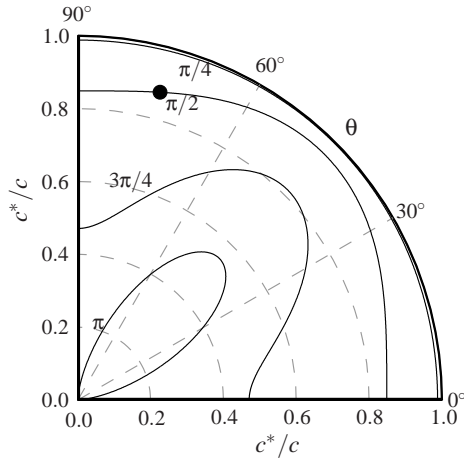Figure 1: Equivalent wavenumber for CDS4 and COM6.

Figure 2: Ratio of numerical phase speed, c^*, to exact phase speed, c, for the fourth order central difference scheme at non-dimensional wavenumbers of $k\Delta = \pi/4$, $\pi/2$, $3\pi/4$, and π, with CFL $= 0.1$CFL$_{max} \approx 0.21$ (CFL$_{max}$ is the maximum CFL for stability).

reveals the *speed* of the wave, and not the *direction* of propagation.

Using an example wave with a non-dimensional wavenumber of $k\Delta = k\Delta_x = \pi/2$ aligned and propagating at $\theta = 75$ degrees, figure 2 shows that the phase velocity ratio is approximately 0.87 as marked by ●. However, as we shall see later, this fails to explain any of the behaviour observed in our numerical experiments. This can only be captured through the use of group velocity [8].

The numerical group velocity in the x and y directions, $u_{g_N} = \frac{\partial \omega_N}{\partial k_x}$ and $v_{g_N} = \frac{\partial \omega_N}{\partial k_y}$ respectively, can be calculated thus [5]

$$\frac{u_{g_N}}{u_{g_{exact}}} = \frac{u_{g_N}}{u} = \frac{-1}{u\Delta_t}\frac{\left(z_r\frac{\partial z_i}{\partial k_x} - z_i\frac{\partial z_r}{\partial k_x}\right)}{|z|^2} \quad (5)$$

$$\frac{v_{g_N}}{v_{g_{exact}}} = \frac{v_{g_N}}{v} = \frac{-1}{v\Delta_t}\frac{\left(z_r\frac{\partial z_i}{\partial k_y} - z_i\frac{\partial z_r}{\partial k_y}\right)}{|z|^2}, \quad (6)$$

where z is the numerical amplitude factor, which is dependent on the equivalent wavenumber and the temporal discretisation method. In this case, the temporal discretisation is fourth order Runge-Kutta, and z is

$$z = 1 - i\Delta_t\left(uk_x^*\Delta_x + vk_y^*\Delta_y\right) + \frac{1}{2}\left(i\Delta_t\left(uk_x^*\Delta_x + vk_y^*\Delta_y\right)\right)^2$$
$$- \frac{1}{6}\left(i\Delta_t\left(uk_x^*\Delta_x + vk_y^*\Delta_y\right)\right)^3 + \frac{1}{24}\left(i\Delta_t\left(uk_x^*\Delta_x + vk_y^*\Delta_y\right)\right)^4. \quad (7)$$

However, unlike phase velocity, group velocity can be negative, which makes it difficult to present on a polar plot such as figure 2. Instead, in figure 3 the x and y group velocities, as calculated using equations (5) and (6), have been converted to velocity magnitude and angle, and the figure 'inverted' so that the contours are the values of group velocity rather than wavenumber, and the axes represent wavenumber rather than phase speed. Figure 3(a) shows the velocity magnitude and figure 3(b) shows the error in the numerical propagation angle, $\theta_{error} = \tan(v_{g_N}/u_{g_N}) - \theta$ for the fourth order central difference scheme.

Returning to the example with a non-dimensional wavenumber of $\pi/2$ aligned and propagating at 75 degrees. This point is marked with ● on figure 3. Referring to figure 3(a) we find that the ratio in velocity magnitude is slightly less than 0.5. Similarly for figure 3(b) we find an error in propagation angle that is slightly more negative than -15 degrees.

Results

This section compares the wave propagation of the two numerical methods under the two-dimensional scalar advection equation

$$\frac{\partial \phi}{\partial t} + u\frac{\partial \phi}{\partial x} + v\frac{\partial \phi}{\partial y} = 0 \quad (8)$$

with the predictions made using group velocity as described above. The numerical experiment uses a two-dimensional grid initialised with a single frequency wave oriented in a particular direction. A Gaussian modulation has also been applied in order to avoid the introduction of high frequency content that arises when there are discontinuities,

$$\phi_0 = e^{-ax^2 + 2bxy + cy^2}\sin\left(k_0(\cos(\theta)x + \sin(\theta)y)\right), \quad (9)$$

where k_0 is the wavenumber, $\theta = \arctan(v/u)$ is the angle the propagation velocity field makes to the x-axis, $a = \cos(\pi/2 - \theta)^2/(2\sigma_x^2) + \sin(\pi/2 - \theta)^2/(2\sigma_y^2)$, $b = -\sin(2(\pi/2 - \theta))/(4\sigma_x^2) + \sin(2(\pi/2 - \theta))/(4\sigma_y^2)$, $c = \sin(\pi/2 - \theta)^2/(2\sigma_x^2) + \cos(\pi/2 - \theta)^2/(2\sigma_y^2)$, $\sigma_x^2 = 1$, and $\sigma_y^2 = 1$. An example of the initial wave with $k_0\Delta = \pi/2$ and $\theta = 75$ degrees is shown in figure 4(a).

The result after four seconds can be seen in the contours of figure 4(b). Also shown in figure 4(b) is a solid arrow, which shows the position of the centre of the wave according to the exact solution. The dashed arrow shows the position of the centre of the wave as predicted by the group velocity. It corresponds well with the numerical result. The solid line is a locus of points that shows the possible range (depending on frequency) of positions for waves aligned with the propagating velocity (i.e. in this case $\theta = 75$ degrees). Note that the only point on this line that is in the same direction as the propagating velocity is at the very top of the line, which corresponds to a non-dimensional wavenumber near zero. Any other waves will not propagate in the direction of the advection field despite being aligned with it.

The result seen here can be related back to the previous discussion on figures 2 and 3. In the former, the ratio of phase velocity magnitude was found to be approximately 0.87; in the latter case the ratio of group velocity magnitude was slightly less than 0.5 and the propagation angle error was approximately -15 degrees. In figure 4(b), we can see that the dashed arrow is approximately half the magnitude of the solid arrow representing the exact solution, and it lies at an angle of 15 degrees less than the exact propagation angle. In comparison, the phase velocity magnitude ratio offers no insight into the numerical result.

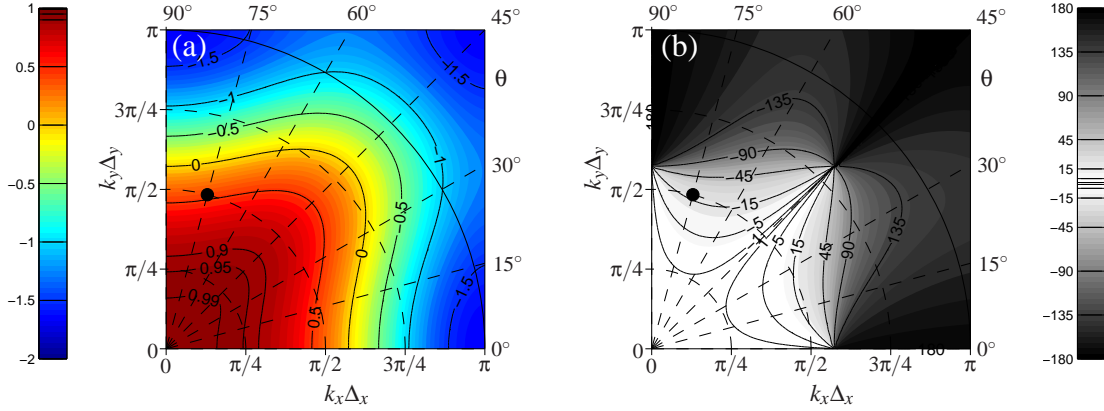A second numerical experiment was conducted in which the ini-

Figure 3: Figures showing (a) the magnitude of the group velocity and (b) the error in propagation angle, for the fourth order central difference scheme with $\lambda = 1$, $\text{CFL} = 0.1\text{CFL}_{\max} \approx 0.21$.
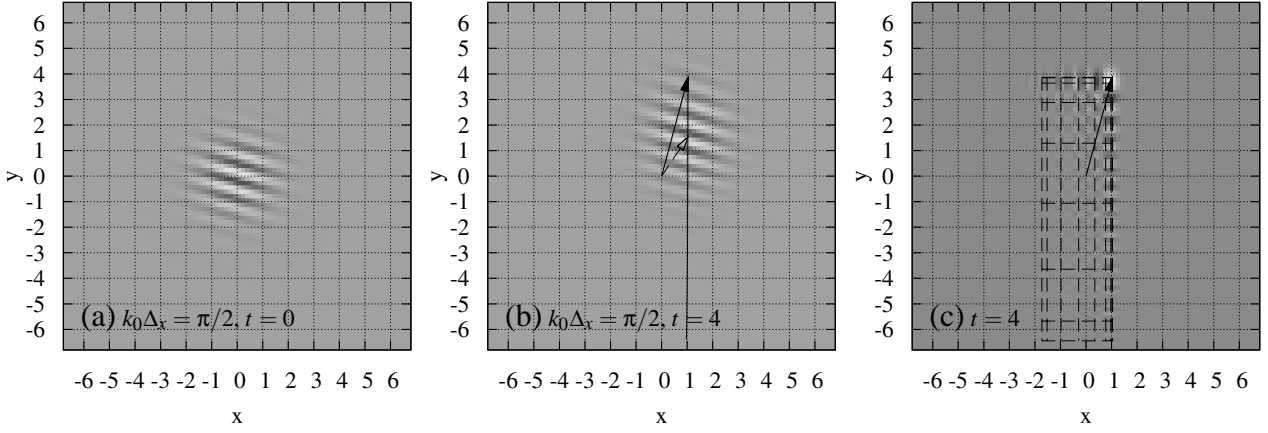

Figure 4: (a) The initial condition: a Gaussian modulated wave of wavenumber $k_0\Delta_x = \pi/2$ aligned at an angle of 75 degrees. (b) The position of the wave shown in (a) after propagating for four seconds with the fourth order central difference scheme in a velocity field of magnitude 1 and direction 75 degrees counter clockwise from the x axis (i.e. $u = 1 \times \cos(75°)$, $v = 1 \times \sin(75°)$). (c) The spread of waves of an initially Gaussian distribution after propagating for four seconds under the same conditions as described in (b). $\text{CFL} = 0.1\text{CFL}_{\max} \approx 0.21$ for both (b) and (c).

tial condition was a Gaussian profile,

$$\phi_0 = e^{-1000(x^2+y^2)}. \tag{10}$$

Unlike the initial condition defined by equation (9), such a profile theoretically contains all frequencies. Therefore, in figure 4(c) the waves of an initial Gaussian profile propagate in all directions. Overlayed on this is a 'grid' of non-dimensional wavenumbers in the x and y directions—$k_x\Delta_x$ and $k_y\Delta_y$ respectively—between 0 and π at increments of $\pi/8$ (with zero corresponding to the upper and rightmost lines). The extent of the grid shows the spread of any possible wave propagation as predicted by the spectral analysis. In comparison with the single line shown on figure 4(b), figure 4(c) shows the case when the wave is not necessarily aligned with the propagating velocity.

In order to show the generality of the analysis, the same analysis has been repeated for two numerical schemes with a propagation angle of 30 degrees. The results are shown in figure 5. The first two rows show the CDS4 scheme, the top row being for a grid aspect ratio of one, i.e. $\lambda = 1$, and the second row for $\lambda = 0.5$. The bottom row shows the COM6 scheme with $\lambda = 1$. The left-most plots show the position of a $k_0\Delta_x = \pi/2$ wave, the centre plots show a $k_0\Delta_x = 3\pi/4$ wave, and the right-most plots show the Gaussian wave.

It can be seen that in each instance, the dashed arrow predictions made by the group velocity are in agreement with the numerical method. It should also be clear that, other than in the well resolved case of figure 5(g), the propagation of the wave is not in the same direction as the propagating velocity.

Whilst the higher resolution scheme COM6 shows improved resolution at low to mid wavenumbers, it has a much larger spread of waves at high wavenumbers, as seen in figure 5(i).

Conclusions

Spectral analysis was used to predict the group velocities for two numerical schemes, and a range of propagation angles and grid aspect ratios. It was found that group velocity as predicted by spectral analysis accurately reflects the results seen from numerical experiments. It was also found that the direction of propagation of waves was not consistent with the advection velocity, regardless of the alignment of the wave. Such behaviour is not reflected in the typical anisotropy diagrams seen in the literature.
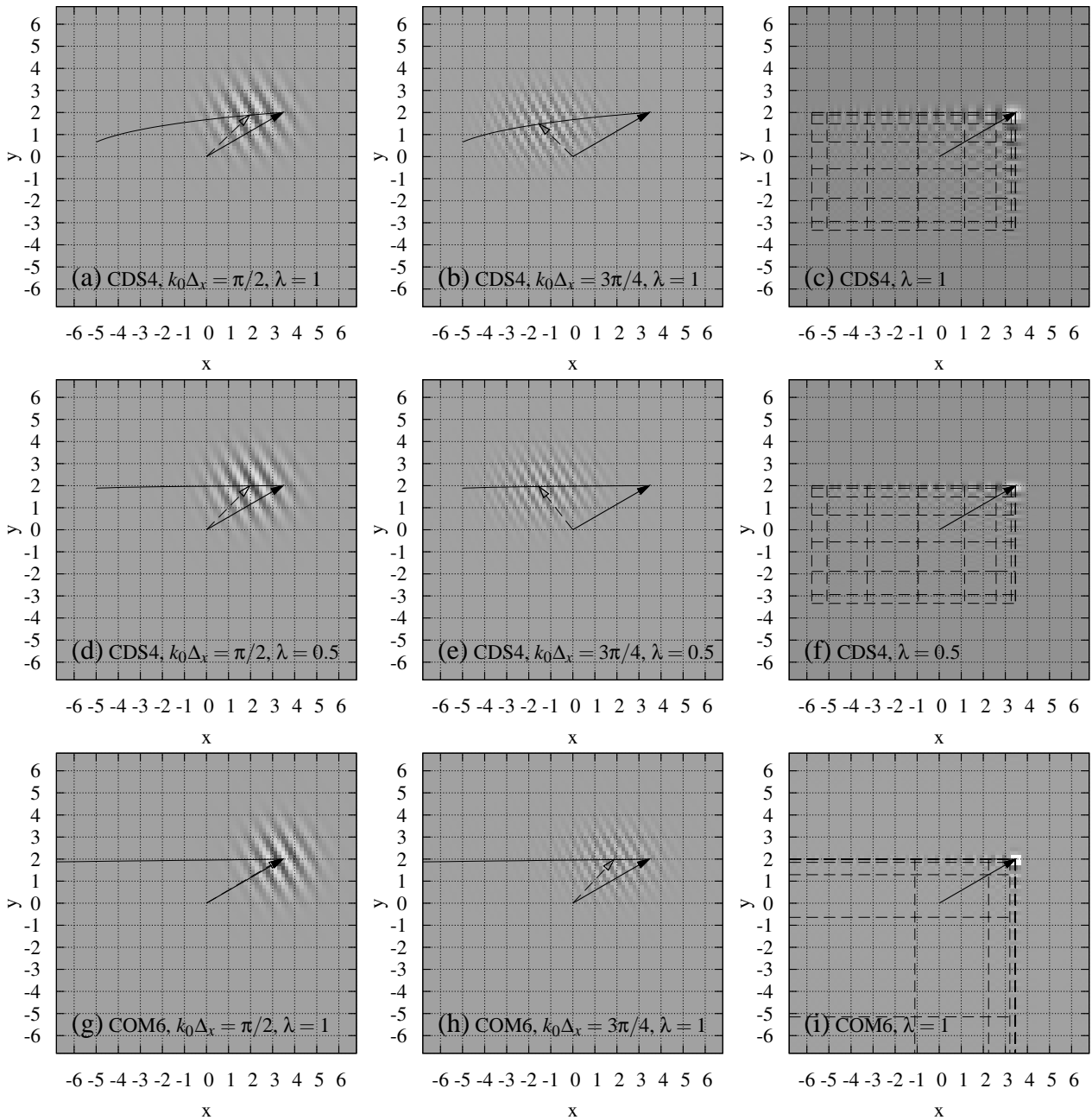
Acknowledgements

Figure 5: Example numerical results overlayed with the position of wave as given by the exact solution and as predicted by the group velocity calculated via the spectral analysis. The first row is the CDS4 scheme with $\lambda = 1$ and $\text{CFL} = 0.1\text{CFL}_{\text{max}} \approx 0.21$; the second row is the CDS4 scheme with $\lambda = 0.5$ and $\text{CFL} = 0.1\text{CFL}_{\text{max}} \approx 0.21$; and the bottom row is the COM6 scheme with $\lambda = 1$ and $\text{CFL} = 0.1\text{CFL}_{\text{max}} \approx 0.14$.

References

[1] Chenoweth, S., Soria, J. and Ooi, A., A new perspective on spectral analysis of numerical schemes, manuscript submitted for publication (April 2010).

[2] Lele, S., Compact finite difference schemes with spectral-like resolution, *J. Comput. Phys.*, **103**, 1992, 16–42.

[3] Li, Y., Wavenumber-extended high order upwind biased finite difference schemes for convective scalar transport, *J. Comput. Phys.*, **133**, 1997, 235–255.

[4] Moin, P., *Fundamentals of Engineering Numerical Analysis*, Cambridge University Press, Cambridge, 2001.

[5] Sengupta, T. and Dipankar, A., A comparative study of time advancement methods for solving Navier-Stokes equations, *J. Sci. Comput.*, **21**, 2004, 225–250.

[6] Sescu, A., Hixon, R. and Afjeh, A., Multidimensional optimization of finite difference schemes for computational aeroacoustics, *J. Comput. Phys.*, **227**, 2008, 4563–4588.

[7] Tam, C. and Webb, J., Dispersion relation preserving finite difference schemes for computational acoustics, *J. Comput. Phys.*, **107**, 1993, 262–281.

[8] Trefethen, L., Group velocity in finite difference schemes, *SIAM Review*, **24**, 1982, 113–136.

[9] Vichnevetsky, R. and Bowles, J., *Fourier Analysis of Numerical Approximations of Hyperbolic Equations*, SIAM, Philadelphia, 1982.